Inorganic Chemistry

Communication

pubs.acs.org/IC

Visual Synchronous Exchange of Metal Nodes and Counteranions Constituting a Cobalt(II) Coordination Polymer

Jian-Cheng Wang, Qi-Kui Liu, Jian-Ping Ma, Fang Huang, and Yu-Bin Dong*

College of Chemistry, Chemical Engineering and Materials Science, Collaborative Innovation Center of Functionalized Probes for Chemical Imaging, Key Laboratory of Molecular and Nano Probes, Ministry of Education, Shandong Normal University, Jinan 250014, P. R. China

Supporting Information

ABSTRACT: A solid-state simultaneous exchange of metal nodes and counteranions based on a cobalt(2+) coordination polymer is reported for the first time. The ion-exchange process is visual, and the structural integrity of the cobalt(2+) coordination polymer is maintained during the ion-exchange process.

Coordination polymers are the species that are constructed from metal nodes and organic spacers.[1] So far, the most effective approach to the synthesis of coordination polymers is self-assembly. In principle, a coordination polymer could be considered as the metal salt of the conjugate base of a weak acid, so the isomorphous replacement of metal nodes by other kinds of metal cations is possible.[2] To date, metal node exchange is rare, although it has been becoming a very useful postsynthetic approach to accessing the coordination polymers that are not easy to be prepare by direct synthesis. To our knowledge, relatively few examples concerning metal node exchange have been reported.[3] On the other hand, among various coordination polymers, cationic coordination polymers often occur when neutral organic ligands are used in construction of the frameworks, so the net positive charge on the frameworks necessitates charge-balancing of extraframework anions. Compared to metal node exchange, anion exchange is much more common. In particular, the simultaneous exchange of metal nodes and counteranions without altering the structural integrity of the framework is hitherto unknown in coordination polymers. Ion exchange (including exchange of metal cations and/or counteranions) based on metal−organic frameworks (MOFs) is of great interest, and such a postsynthetic approach[4] might be able to conveniently modify or improve MOF functions under ambient conditions.

In this contribution, we report for the first time the synchronous metathesis of both metal nodes and counterions based on a 1D cobalt(2+) coordination polymer.

$Co_2L_2Cl_2$ (**1**) was obtained as purple crystals by the combination of L and $CoCl_2$ in a mixed-solvent system of CH_2Cl_2/methanol (MeOH) at ambient temperature (Scheme 1). Single-crystal X-ray diffraction analysis revealed that the 1D coordination polymer of **1** (Figure S1 in the Supporting Information, SI) crystallizes in the triclinic space group $P\bar{1}$. As shown in Figure 1, each Co^{2+} node in **1** adopts a distorted octahedral $\{CoN_4Cl_2\}$ coordination sphere. The basal plane is composed of two *N*-pyrimidyl [d_{Co-N} = 2.212(5) Å] and two *N*-pyridyl [d_{Co-N} = 2.244(6) Å] donors. The axial positions are occupied by two coordinated Cl^- anions [d_{Co-Cl} = 2.388(2) Å]. Compound **1** is stable in air as well as in MeOH (Figure S1 in the SI).

Scheme 1. Synthesis of 1

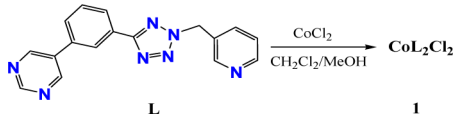

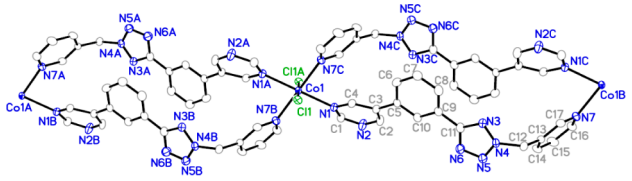

Figure 1. ORTEP figure of **1** (displacement ellipsoids drawn at the 30% probability level).

Metal node exchange based on **1** was simply realized by the combination of **1** with Cu^{2+} in solution. As shown in Scheme 2, when compound **1** was soaked in a MeOH solution of $CuCl_2$ (0.02 mol/L) for 30 min, the crystals of **1** underwent a rapid naked-eye-detectable color change. As illustrated in Scheme 2,

Scheme 2. Synthesis of 2−4 Based on Metal Nodes and Counter Ions Exchange[a]

[a]The photographs of **1**−**4** and their formation process are inset.

Received: June 7, 2014
Published: September 26, 2014

the color of the resulting crystalline solids of $Cu_{0.74}Co_{0.26}L_2Cl_2$ (**2**) gradually changed from purple to green, which is further supported by the UV−vis spectrum (Figure S2 in the SI). Unfortunately, the crystals of **1** did not diffract the X-ray beams due to the loss of single crystallinity during the process. The powder X-ray diffraction (PXRD) pattern based on **2**, however, is identical with that of **1**, indicating that the structural integrity is maintained (Figure 2), so the color change of **1** resulted from

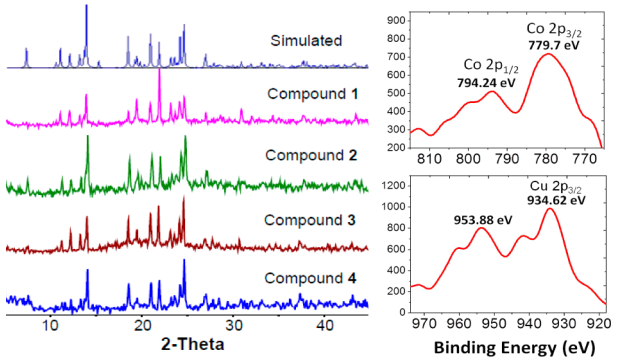

Figure 2. (Left) PXRD patterns of **1**−**4**. (Right) XPS spectra of **2**.

metal node exchange. The coexistence of Co^{2+} and Cu^{2+} in **2** is further demonstrated by X-ray photoelectron spectroscopy (XPS) measurement, which is evidenced by the observation of Co $2p_{3/2}$ (at 779.7 eV), Co $2p_{1/2}$ (at 794.24 eV),[5] and Cu $2p_{3/2}$ (at 934.62 eV)[6] peaks in the XPS spectra of **2** (Figure 2). The metal-cation-exchange degree in **1** was determined by inductively coupled plasma (ICP) measurement. The ICP-measured result (Table S1 and Figure S3 in the SI) indicates that the amount of Cu^{2+} is up to ca. 75%, which is in accordance with the molecular formula of $Cu_{0.74}Co_{0.26}L_2Cl_2$.

To provide further insight into metal node exchange based on **1**, $CuBr_2$ and $Cu(NO_3)_2$ were used instead of $CuCl_2$ to perform the ion-exchange reactions under the same conditions. By simply immersion of the crystals of **1** in a MeOH solution (0.02 mol/L) of $CuBr_2$ for 3 h, the color of **1** stepwise-changed from purple to dark brown to generate $Cu_{0.98}Co_{0.02}L_2ClBr$ (**3**; Scheme 2 and Figure S3 in the SI). Notably, XPS measurements (Figure 3)

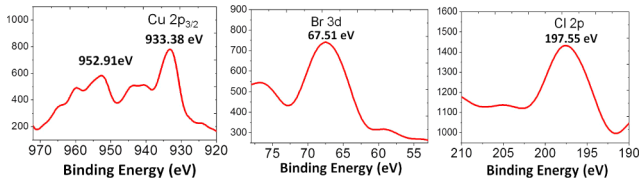

Figure 3. XPS spectra of **3**. No detectable Co^{2+} species was observed.

show that compound **3** contains not only Cu^{2+} (Cu $2p_{3/2}$ at 933.38 eV)[6] and Cl^- (Cl 2p at 197.55 eV)[7] species but also the Br^- (Br 3d at 67.51 eV) anion,[7] which means that both Co^{2+} nodes and the Cl^- counteranions in **1** were simultaneously replaced by Cu^{2+} and Br^-. Interestingly, no obvious peaks related to Co^{2+} were observed based on XPS, indicating that almost all Co^{2+} cations in **1** are exchanged by Cu^{2+}. The ICP measurement (Table S2 and Figure S4 in the SI) shows that the amount of Cu^{2+} is up to ca. 98%, and ion chromatography (IC) analysis of the amount of Cl^- ions is ca. 50% (see the SI). So, the structural formula of compound **3** should be $Cu_{0.98}Co_{0.02}L_2ClBr$. Again, the framework structural integrity of **1** is maintained, which is well demonstrated by the measured PXRD pattern (Figure 2).

For $Cu(NO_3)_2$, as illustrated in Scheme 2, the color of **1** changed from purple to sky blue after **1** was immersed in a MeOH solution (0.02 mol/L) of $Cu(NO_3)_2$ for 12 h (Figure S5 in the SI). The Cu $2p_{3/2}$ (at 933.71 eV)[6] and Cl 2p (at 197.78 eV)[7] peak positions are in accordance with the presence of Cu^{2+} and Cl^- ions (Figure 4), respectively. Similar to **3**, no Co^{2+}

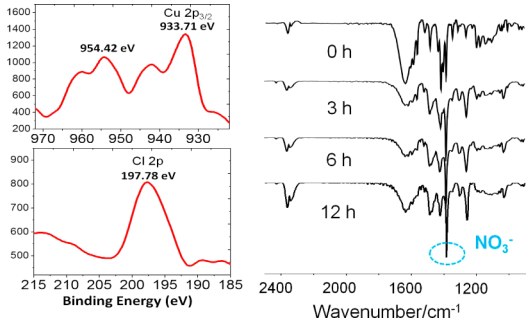

Figure 4. (Left) XPS spectra of **4**. No detectable Co^{2+} species was observed. (Right) IR spectra recorded during the ion-exchange process at 0−12 h.

species was detected in **4** based on XPS measurement, indicating that the Co^{2+} ion in **1** was completely replaced by Cu^{2+}. On the other hand, IR spectra show that the bands associated with NO_3^- are significantly enhanced as time goes on, indicating that the Cl^- ion in **1** was exchanged by the incursive nitrate anions (Figure 4). The ICP measurements (Table S3 and Figure S6 in the SI) reveal that ca. 100% of Co^{2+} cations in **1** were replaced by Cu^{2+} cations; meanwhile, ca. 35% of Cl^- anions were exchanged by the NO_3^- anions. So, the ion-exchange reaction yields compound **4** with a molecular formula of $CuL_2Cl_{1.3}(NO_3)_{0.7}$. The PXRD pattern based on the ion-exchanged sample of **4** is identical with that of **1** (Figure 2), suggesting that the framework is intact upon ion exchange.

Notably, no ligand species were detected in mother liquors of **2**−**4** based on the ^1H NMR spectrum during the process (Figure S7 in the SI), indicating that the above visual synchronous metathesis of metal nodes and counteranions based on **1** is a solid-state ion exchange. To further confirm this, liquid chromatography (LC) was used to monitor the mother liquors of **2**−**4**. For **2** and **3**, no ligand was present in the mother liquors based on LC analysis; for **4**, only a tiny amount of ligand was detected, indicating that compound **4** is slightly soluble in MeOH (Figure S8 in the SI).

It is noteworthy that the copper(2+) coordination polymers with the same structure of **1** cannot be obtained by the direct combination of L and corresponding CuX (X = Cl^-, Br^-, and NO_3^-) salts in $MeOH/CH_2Cl_2$ (Figure S9 in the SI) and other solvent systems such as $EtOH/CH_2Cl_2$, CH_3CN/CH_2Cl_2, $MeOH/CHCl_3$, $EtOH/CHCl_3$, MeOH/THF, and H_2O/MeOH. Notably, the metal node and counteranion exchanges herein are irreversible under the experimental conditions. In addition, ion exchange did not occur when $CuSO_4$, $Cu(OAc)_2$, and $Cu(SO_3CF_3)_2$ were used to perform the reactions under the same conditions.

Notably, the ion-exchange reaction time of **1** based on the different CuX_2 (X = Cl^-, Br^-, and NO_3^-) salts was monitored by PXRD. The ion-exchange time exceeded 0.5 h (for **2**), 3 h (for **3**), and 12 h (for **4**); the solid-state structure of **1** could not be

dx.doi.org/10.1021/ic5013186 | Inorg. Chem. 2014, 53, 10791−10793

maintained based on the PXRD measurement. As mentioned above, the ion-exchange rate of these reactions is quite different.[8] For example, the naked-eye-detectable color change from **1** to **2** was observed in ∼1 min, while the color changes from **1** to **3** and from **1** to **4** were observed in 0.5 and 1 h, respectively. All of the reaction conditions, including starting materials, solvents, and temperature, are the same except anions, so the different ion-exchange rates herein might be caused by the different anions. For further understanding the different ion-exchange rates caused by the different metal salts, DFT calculations were carried out. The calculations were carried out using *Gaussian 09* at the M06 level. A 6-31G* basis set was employed for Cl, Br, N, and O atoms. For Cu and Co atoms, the standard LanL2DZ was used. $CoCl_2$, $CuCl_2$, $CoBr_2$, $CuBr_2$, $Co(NO_3)_2$, and $Cu(NO_3)_2$ were fully optimized. Single-point calculation of $CoCl_2L_2$ was performed based on its X-ray crystal structure. Because the PXRD measurements gave the same structural information for $CuCl_2L_2$, $CuBr_2L_2$, $CoBr_2L_2$, $Cu(NO_3)_2L_2$, and $Co(NO_3)_2L_2$, Co−Cl bonds in $CoCl_2L_2$ were replaced by Cu−Cl, Cu−Br, Co−Br, Cu−NO_3, and Co−NO_3 bonds, giving the structures of $CuCl_2L_2$, $CuBr_2L_2$, $CoBr_2L_2$, $Cu(NO_3)L_2$, and $Co(NO_3)L_2$. Then electronic energies of $CuCl_2L_2$, $CuBr_2L_2$, $CoBr_2L_2$, $Cu(NO_3)_2L_2$, and $Co(NO_3)_2L_2$ were obtained from optimization of the Cu−Cl, Cu−Br, Co−Br, Cu−NO_3, and Co−NO_3 moieties with metal−L parts frozen. The electronic energies were further improved by single-point calculation, with solvent effects (SCRF = IEFPCM and solvent = MeOH) taken into account. According to the calculations, the electronic energy changes of the three reactions [$CuCl_2 + CoCl_2L_2 \rightarrow CoCl_2 + CuCl_2L_2$ (1); $CuBr_2 + CoCl_2L_2 \rightarrow CoCl_2 + CuBr_2L_2$ (2); $Cu(NO_3)_2 + CoCl_2L_2 \rightarrow CoCl_2 + Cu(NO_3)_2L_2$ (3)] are −2.4(1), 16.3(2), and 19.6(3) kcal/mol, which are in good agreement with the observations of the above ion-exchange reactions.

In summary, we have successfully demonstrated, for the first time, a simultaneous exchange of metal nodes and counteranions on the coordination polymers in the solid state. The facile exchange of metal nodes and counterions without loss of structural integrity as described herein might provide an alternative approach to constructing heterometallic and heteroanionic coordination polymer materials with the same framework structural feature under ambient conditions. On the other hand, such interesting naked-eye-detectable ion-responsive color changes might be useful in visual sensors for the detection of metal cations and counteranions.

■ ASSOCIATED CONTENT

Supporting Information

Synthesis and characterization data for the ligand and **1**−**4**, including figures and tables for ORTEP, crystal packing, ICP, IC analysis, UV−vis spectra, LC analysis, a CIF file, and crystal data. This material is available free of charge via the Internet at http://pubs.acs.org.

■ AUTHOR INFORMATION

Corresponding Author

*E-mail: yubindong@sdnu.edu.cn.

Notes

The authors declare no competing financial interest.

■ ACKNOWLEDGMENTS

We are grateful for financial support from the 973 Program (Grant 2012CB821705), NSFC (Grants 21271120 and 21101100), and "PCSIRT".

■ REFERENCES

(1) Leong, W. L.; Vittal, J. J. *Chem. Rev.* **2011**, *111*, 688−764.

(2) Lalonde, M.; Bury, W.; Karagiaridi, O.; Brown, Z.; Hupp, J. T.; Farha, O. K. *J. Mater. Chem. A* **2013**, *1*, 5453−5468 and references cited therein.

(3) So far, some typical examples for metal node exchange based on coordination polymers in the solid state have been reported. See: (a) Dincă, M.; Long, J. R. *J. Am. Chem. Soc.* **2007**, *129*, 11172−11176. (b) Brozek, C. K.; Dinca, M. *Chem. Sci.* **2012**, *3*, 2110−2113. (c) Li, J.; Li, L.; Hou, H.; Fan, Y. *Cryst. Growth Des.* **2009**, *9*, 4504−4513. (d) Botas, J. A.; Calleja, G.; Sánchez-Sánchez, M.; Orcajo, M. G. *Langmuir* **2010**, *26*, 5300−5303. (e) Denysenko, D.; Werner, T.; Grzywa, M.; Puls, A.; Hagen, V.; Eickerlinbg, G.; Jelic, J.; Reuter, K.; Volkmer, D. *Chem. Commun.* **2012**, *48*, 1236−1238. (f) Mi, L.; Hou, H.; Song, Z.; Han, H.; Xu, H.; Fan, Y.; Ng, S.-W. *Cryst. Growth Des.* **2007**, *7*, 2553−2561. (g) Das, S.; Kim, H.; Kim, K. *J. Am. Chem. Soc.* **2009**, *131*, 3814−3815. (h) Cairns, A. J.; Perman, J. A.; Wojtas, L.; Kravtsov, V. C.; Alkordi, M. H.; Eddaoudi, M.; Zoworotko, M. J. *J. Am. Chem. Soc.* **2008**, *130*, 1560−1561. (i) Zhang, Z.-J.; Shi, W.; Niu, Z.; Li, H.-H.; Zhao, B.; Cheng, P.; Liao, D.-Z.; Yan, S.-P. *Chem. Commun.* **2011**, *47*, 6425−6427. (j) Kim, M.; Cahill, J. F.; Fei, H.; Prather, K. A.; Cohen, S. M. *J. Am. Chem. Soc.* **2012**, *134*, 18082−18088. (k) Mukherjee, G.; Biradha, K. *Chem. Commun.* **2012**, *48*, 4293−4295. (l) Prasad, T. K.; Hong, D. H.; Suh, M. P. *Chem.—Eur. J.* **2010**, *16*, 14043−14050. (m) Yao, Q.; Sun, J.; Li, K.; Su, J.; Peskov, M. V.; Zou, X. *Dalton Trans.* **2012**, *41*, 3953−3955. (n) Wei, Z.; Lu, W.; Jiang, H.-L.; Zhou, H.-C. *Inorg. Chem.* **2013**, *52*, 1164−1166. (o) Shultz, A. M.; Sarjeant, A. A.; Farha, O. K.; Hupp, J. T.; Nguyen, S. B. T. *J. Am. Chem. Soc.* **2011**, *133*, 13252−13255. (p) Zhang, Z.; Zhang, L.; Wojtas, L.; Nugent, P.; Eddaoudi, M.; Zaworotko, M. J. *J. Am. Chem. Soc.* **2011**, *134*, 924−927. (q) Zhang, Z.; Gao, W.-Y.; Wojtas, L.; Ma, S.; Eddaoudi, M.; Zaworotko, M. J. *Angew. Chem., Int. Ed.* **2012**, *51*, 9330−9334. (r) Morris, W.; Volosskiy, B.; Demir, S.; Gándara, F.; McGrier, P. L.; Furukawa, H.; Cascio, D.; Stoddart, J. F.; Yaghi, O. M. *Inorg. Chem.* **2012**, *51*, 6443−6445.

(4) (a) Wang, Z.; Cohen, S. M. *Chem. Soc. Rev.* **2009**, *38*, 1315−1329. (b) Song, Y.-F.; Cronin, L. *Angew. Chem., Int. Ed.* **2008**, *47*, 4635−4637. (c) Tanabe, K. K.; Cohen, S. M. *Chem. Soc. Rev.* **2011**, *40*, 498−519.

(5) Jia, C.-J.; Schwick, M.; Weidenthaler, C.; Schmidt, W.; Korhonen, S.; Weckhuysen, B. M.; Schüth, F. *J. Am. Chem. Soc.* **2011**, *133*, 11279−11288.

(6) (a) Balamurugan, B.; Mehta, B. R.; Shivaprasad, S. M. *Appl. Phys. Lett.* **2001**, *79*, 3176−3178. (b) Huang, Y. G.; Mu, B.; Schoenecker, P. M.; Carson, C. G.; Karra, J. R.; Cai, Y.; Walton, K. S. *Angew. Chem., Int. Ed.* **2011**, *50*, 436−440.

(7) Ma, J.-P.; Yu, Y.; Dong, Y.-B. *Chem. Commun.* **2012**, *48*, 2946−2948.

(8) (a) Song, X.; Kim, T. K.; Kim, H.; Kim, D.; Jeong, S.; Moon, H. R.; Lah, M. S. *Chem. Mater.* **2012**, *24*, 3065−3073. (b) Song, X.; Jeong, S.; Kim, D.; Lah, M. S. *CrystEngComm* **2012**, *14*, 5753−5756.